Modeling of Cyborg-Cockroach Swarm Using Agent-Based Simulation

Le Minh Triet and Nguyen Truong Thinh *

Institute of Intelligent and Interactive Technologies, University of Economics Ho Chi Minh City - UEH, Vietnam
Email: lmt30062003@gmail.com (L.M.T.), thinhnt@ueh.edu.vn (N.T.T.)
*Corresponding author

Abstract—This study investigates the behavior and performance of Cyborg Insect Swarms operating under a decentralized control mechanism. Cyborg insects, which integrate living insects with miniature electronic controllers, represent an innovative approach in swarm robotics, combining biological capabilities with artificial control systems. We utilized the Multi-agent Robot Swarm Simulation (MARSS) platform to model and analyze the dynamics of these hybrid entities in various simulated environments and scenarios. The research aimed to understand how cyborg insect swarms perform compared to traditional robotic swarms, particularly in terms of adaptability, efficiency, and coordination in complex tasks. We conducted extensive simulations replicating diverse environmental conditions and task requirements to assess swarm behavior, inter-agent communication, and overall swarm efficiency. The study focused on key performance metrics including task completion time, energy efficiency, and adaptability to unexpected obstacles or changing objectives. Results demonstrated that cyborg insect swarms exhibited enhanced flexibility and adaptability in complex and dynamic environments, effectively leveraging the natural sensory capabilities and agility of insects. The bio-hybrid nature of the swarm allowed for more nuanced responses to environmental stimuli compared to fully artificial systems. However, the research also revealed challenges unique to cyborg swarms, particularly in maintaining consistent swarm behavior due to the inherent biological variability among individual insects. Despite these challenges, the study highlighted potential advantages of cyborg insect swarms in applications such as environmental monitoring, disaster response, and search-and-rescue operations. These findings contribute significantly to the emerging field of bio-hybrid systems and provide valuable insights into the practical implementation and potential real-world applications of cyborg insect swarms.

Keywords—cyborg insect swarm, bio-hybrid systems, decentralized control, swarm robotics, multi-agent simulation, Multi-agent Robot Swarm Simulation (MARSS) platform, swarm behavior, adaptive control

I. INTRODUCTION

The use of robotic swarms has gained significant attention in recent years, particularly in scenarios such as search and rescue operations, where human intervention in narrow or hazardous environments is both challenging and dangerous [1]. In this context, robotic swarm technologies have the potential to reduce risks to human operators while performing essential tasks. Recent advancements in bio-hybrid systems, such as cyborg insects—living insects augmented with controllers—offer promising alternatives to purely mechanical robots [2]. These bio-hybrid systems utilize the insects' natural mobility, combined with artificial control mechanisms, making them highly adaptable to complex environments.

While individual cyborg insects have been the focus of research for several years [3], studies on swarms of cyborg insects functioning collectively remain scarce. Addressing this gap could significantly advance the field, as cyborg insect swarms have the potential to offer increased energy efficiency and adaptability compared to fully robotic systems [4]. Furthermore, the decentralized control of such swarms would allow for autonomous decision-making based on sensory inputs from the insects themselves, eliminating the need for constant manual intervention [5].

Despite these advancements, developing and maintaining large-scale swarms remains resource-intensive, with hardware modifications often proving costly for experimental purposes. Therefore, simulation platforms have emerged as an essential tool for modeling swarm behaviors and optimizing designs before physical implementation [6]. In the context of cyborg cockroach systems, modeling and simulation can provide insights into swarm dynamics, helping to identify optimal configurations and reducing the need for extensive physical testing. This approach follows recent trends in swarm robotics research, where simulations are employed to explore key parameters and trade-offs before deploying physical systems [7]. We have utilized a custom Multi-agent Robot Swarm Simulation (MARSS) platform, developed in Processing, to model cyborg-cockroach swarms. MARSS is an agent-based framework tailored for biohybrid systems, enabling the simulation of *Periplaneta americana (P.americana)* agents with detailed kinematics, decentralized swarm behaviors, and interactive 3D environments. Key features include real-time visualization, collision detection, pheromone-based coordination, and support for integrating natural insect traits with electronic control, such as neural stimulation responses. Built for this research, MARSS facilitates the

analysis of adaptability and efficiency in complex scenarios, bridging biological and robotic paradigms for applications like search-and-rescue and environmental monitoring. By leveraging MARSS, we simulate the swarm's adaptability and efficiency under decentralized rules, providing a robust foundation for analyzing biohybrid systems in diverse scenarios, such as aggregation and collective task execution.

This study aims to address the gap in the research on cyborg insect swarms by developing models of cyborg cockroach swarms using decentralized control mechanisms. These models will help to better understand the potential applications of bio-hybrid swarms in areas such as search and rescue, environmental monitoring, and precision agriculture [8]. By focusing on simulation, we aim to contribute to the broader field of swarm robotics and bio-hybrid systems, providing a cost-effective means of exploring these complex systems.

II. BEHAVIORS OF CYBORG-COCKROACH

The American cockroach—*P.americana*—is one of the largest species of common cockroaches, known for its remarkable survival abilities and adaptability. This species exhibits several key characteristics that make it an ideal candidate for cyborg applications, aligning with the growing field of bio-hybrid robots [9]. Adult specimens typically range from 28 to 44 mm in length, with males being slightly smaller than females. The species is characterized by a reddish-brown coloration and a distinctive yellowish figure-eight pattern on the pronotum. It possesses two pairs of wings: leathery forewings (tegmina) and membranous hindwings, allowing for flight in certain conditions. The cockroach's three pairs of legs are equipped with numerous sensory and locomotory spines that contribute to its remarkable mobility and environmental awareness. Its long, filiform antennae, extending up to 5 cm, serves as highly sensitive sensory organs, while the short, articulated cerci at the rear detect air movements, providing an additional layer of environmental perception. *P.americana* is known for its remarkable locomotion, making it one of the fastest insects relative to body size. It can achieve speeds of up to 5.4 km/h (3.4 mph) and exhibits impressive agility, capable of making sharp turns while maintaining speed and maneuvering through complex terrains with ease. This agility has made it a popular choice for bio-hybrid robotic systems, as demonstrated in recent studies [10]. Equipped with specialized tarsal pads, it can effortlessly scale vertical surfaces and even traverse ceilings. Additionally, its highly evolved escape response, with a latency of approximately 40 to 50 ms, allows it to react swiftly to perceived threats, making it highly elusive in the face of danger. This cockroach species possesses highly developed sensory capabilities, which significantly enhance its adaptability. Its compound eyes are sensitive to changes in light intensity and movement, allowing for acute visual perception. Mechanoreceptive hairs on its body and legs provide heightened sensitivity to vibrations and physical stimuli. The antennae are equipped with numerous chemoreceptors, enabling the detection of odors and pheromones crucial for navigation and communication. Additionally, cockroaches possess advanced thermoreception, the ability to sense subtle temperature changes in their surroundings through specialized receptors, which enhances their adaptability and awareness across diverse conditions. This sensory trait has been harnessed in cyborg insect research, including our agent-based simulation, where it informs swarm behavior—such as avoiding extreme heat zones—and underscores the potential for sophisticated bio-hybrid sensory systems [11].

This species exhibits extraordinary survival adaptations, contributing to its resilience in a wide range of environments. It can endure up to a month without food and survive for two weeks without water, showcasing its remarkable ability to tolerate deprivation. Additionally, it demonstrates significant radiation resistance, tolerating doses up to 15 times higher than the lethal threshold for humans. Its ability to survive without oxygen for 40 min and hold its breath for 5 to 7 min further enhances its adaptability, enabling it to thrive under conditions that would be fatal to many other organisms. These survival traits make P. americana an excellent candidate for cyborg applications in hazardous environments, as explored in recent research [12].

The nervous system of *P.americana* is a complex and decentralized network that allows for rapid information processing and response. Understanding this system is crucial for effective cyborg control, as highlighted in several studies on insect-machine interfaces [13]. The central nervous system of this species is intricately structured to efficiently manage sensory input and motor coordination. At the core is the brain, or supraesophageal ganglion, located above the esophagus. It comprises three distinct ganglia—the protocerebrum, deutocerebrum, and tritocerebrum—that work together to process complex sensory data, orchestrate motor responses, and regulate higher-order behaviors such as decision-making and navigation. Below the esophagus, key nerve cluster called the subesophageal ganglion, located just below the esophagus in the head, regulates essential activities tied to feeding and movement. This structure controls the mouthparts, salivary glands, and neck muscles, ensuring coordinated behavior that we model in our cyborg-cockroach swarm simulation. Extending along the ventral side of the body is the ventral nerve cord, which serves as the primary communication pathway between the brain and peripheral nervous system. It houses thoracic and abdominal ganglia, with the thoracic ganglia (in three pairs) responsible for controlling leg movements and wing muscles, facilitating precise locomotion and flight. Meanwhile, the six pairs of abdominal ganglia govern critical abdominal functions and the movement of posterior appendages, ensuring smooth coordination of both voluntary and involuntary actions across the body. This decentralized nervous system architecture has been leveraged in recent cyborg cockroach studies to achieve more precise control over locomotion and behavior [14].

The peripheral nervous system plays a crucial role in linking the body's sensory inputs with motor outputs,

facilitating seamless interaction with the environment. Sensory neurons are responsible for transmitting information from various sensory organs to the central nervous system. These include specialized receptors such as mechanoreceptors for detecting physical forces, chemoreceptors for sensing chemical stimuli like odors, thermoreceptors for temperature changes, and photoreceptors for light detection. On the output side, motor neurons relay signals from the central nervous system to muscles and glands, enabling coordinated movements and physiological responses that allow the organism to adapt and react to its surroundings with precision. The integration of these sensory systems into cyborg designs has led to innovative applications in environmental sensing and monitoring [15].

The nervous system of this species features several key characteristics that enhance its adaptability and survival. One of the most prominent aspects is its decentralized control, where each ganglion can independently process information and generate responses. This autonomy allows for rapid local reflexes, bypassing the need for brain involvement and enabling quicker reactions to stimuli. The giant fiber system, consisting of large-diameter axons, is particularly important for facilitating rapid signal transmission, crucial for the species' swift escape responses. This architecture ensures that reaction times to threats are almost instantaneous, a feature that has been exploited in recent cyborg designs for rapid obstacle avoidance and navigation [16].

Neuromodulation plays a significant role in fine-tuning neural circuits, with key neurotransmitters and modulators such as acetylcholine, Gamma-Aminobutyric Acid (GABA)—an inhibitory neurotransmitter calming neural signals, octopamine, and serotonin shaping various physiological and behavioral responses. Additionally, the cockroach nervous system demonstrates a degree of neuroplasticity, allowing for adaptation and learning over time. This plasticity enhances the species' ability to adjust its behavior in response to environmental changes, further contributing to its remarkable resilience. Recent studies have explored the potential of leveraging this neuroplasticity in cyborg systems to create more adaptive and learning-capable bio-hybrid robots [17].

Understanding the kinematics of cockroach locomotion is essential for developing effective control strategies in cyborg applications, as demonstrated in several recent studies [18]. The American cockroach employs a variety of gaits and can rapidly transition between them based on speed and environmental conditions. The legs of this species are intricately structured to optimize locomotion and maneuverability. Each of the six legs is composed of five primary segments, each serving a specific function. The coxa attaches the leg to the body, allowing for rotational movement both forward and backward. The trochanter, a small segment located between the coxa and the femur, assists in the nuanced movement of the leg. The femur is the largest segment and plays a crucial role in generating the power necessary for locomotion. The tibia works in concert with the femur to facilitate movement and is equipped with sensory spines that

contribute to the insect's tactile feedback and environmental awareness. Finally, the tarsus, or foot, is multi-segmented and features claws and adhesive pads that enhance grip and stability on various surfaces, aiding in climbing and traction.

This species employs distinct gait patterns to optimize movement across different speeds and terrains, which have been extensively studied and modeled for cyborg locomotion control [19]: *Tripod Gait:* The primary walking gait involves having three legs in contact with the ground at any given time. This gait alternates between two tripods: (R1, L2, R3) and (L1, R2, L3), where R and L denote right and left legs, respectively, and 1, 2, and 3 indicate the front, middle, and hind legs. The frequency of this gait ranges from 2 to 8 Hz, depending on the walking speed, providing a stable and efficient means of locomotion. *Metachronal Wave Gait*: At slower speeds, below 10 cm/s, the cockroach utilizes a metachronal wave gait. In this pattern, the legs move in a sequential back-to-front motion on each side of the body, which helps maintain stability and smooth movement at lower velocities. *Running Gait*: When speeds exceed 50 cm/s, the cockroach transitions to a running gait. This gait is characterized by aerial phases during which all legs are momentarily off the ground. This allows for rapid and agile movement, enabling the cockroach to navigate quickly through its environment. The diverse locomotion capabilities of *P.americana*, combined with its robust sensory systems and adaptability, make it an excellent platform for cyborg applications. Recent advancements in miniaturized electronics and neurostimulation techniques have further enhanced the potential of cockroach-based cyborgs for applications ranging from search and rescue operations to environmental monitoring [20]. As research in this field continues to progress, the integration of biological systems with artificial control mechanisms promises to yield increasingly sophisticated and capable bio-hybrid robots. The kinematics of each cockroach leg is modeled using a three-segment system consisting of the coxa, femur, and tibia. Each segment is characterized by its length (l_c, l_f, l_t) and mass (m_c, m_f, m_t). The joint angles between these segments are defined as θ_c (coxa-body), θ_f (coxa-femur), and θ_t (femur-tibia):

$$\begin{bmatrix} x \\ y \\ z \end{bmatrix} = \begin{bmatrix} l_c \cos\theta_c + l_f \cos(\theta_c + \theta_f) + l_f \cos(\theta_c + \theta_f + \theta_t) \\ l_c \sin\theta_c + l_f \sin(\theta_c + \theta_f) + l_f \sin(\theta_c + \theta_f + \theta_t) \\ l_f \cos\theta_f + l_f \sin(\theta_f + \theta_t) \end{bmatrix} \quad (1)$$

The temporal evolution of joint angles is modeled using a sinusoidal function to approximate the rhythmic nature of cockroach locomotion:

$$\theta_c(t) = A_i \sin(2\pi f_i t + \phi_i) + \theta_{i,0} \quad (2)$$

where $i \in \{c, f, t\}$, A_i is the amplitude, f_i is the frequency, ϕ_i is the phase offset, and $\theta_{i,0}$ is the mean angle for each joint. The body's center of mass (*CoM*) motion is derived

from the leg movements. Assuming a tripod gait, the body velocity **v** is approximated by:

$$v(t) = \frac{1}{3} \sum_{j \in S(t)} \frac{dp_j}{dt} \quad (3)$$

where $S(t)$ is the set of legs in contact with the ground at time t, and $\mathbf{p}_j$ is the position of the j-th leg's endpoint relative to the body. Body orientation is updated using quaternion rotation to avoid gimbal lock:

$$q(t + \Delta t) = q(t) \otimes \exp(\frac{1}{3} \omega \Delta t) \quad (4)$$

where q is the orientation quaternion, ω is the angular velocity, and $\otimes$ denotes quaternion multiplication. The cyborg enhancement is modeled as an additional term in the joint angle equations:

$$\theta_c(t) = A_i \sin(2\pi f_i t + \phi_i) + \theta_{i,0} + K_i S_i(t) \quad (5)$$

where K_i is the gain for joint i, and $S_i(t)$ is the stimulation signal. The stimulation signal is modeled as a pulse train:

$$S_i(t) = A_s \sum_k rect(\frac{t - kT_s}{\tau_s}) \quad (6)$$

where A_s is the stimulation amplitude, T_s is the stimulation period, τ_s is the pulse width, and $rect$ is the rectangular function. Collision avoidance between agents is modeled using a repulsive force:

$$F_{rep,ij} = \begin{cases} k_{rep}(\frac{1}{|r_{ij}|} - \frac{1}{r_0})\frac{r_{ij}}{|r_{ij}|^2} & if \; |r_{ij}| < r_0 \\ 0 & otherwise \end{cases} \quad (7)$$

where r_{ij} is the vector from agent i to agent j, k_{rep} is the repulsion strength, and r_0 is the interaction radius. Alignment and cohesion are modeled using the Vicsek model:

$$\theta_i(t + \Delta t) = \langle \theta_i(t) \rangle_{j \in N_i} + \Delta \theta_i \quad (8)$$

where $\langle . \rangle_{j \in N_i}$ denotes the average over the neighbors N_i of agent i, and $\Delta\theta_i$ is a noise term. The overall swarm behavior emerges from the combination of individual kinematics and inter-agent interactions. We quantify swarm cohesion using the average distance to the swarm's center of mass:

$$C(t) = \frac{1}{N} \sum_{i=1}^{N} |r_i(t) - r_{CM}(t)| \quad (9)$$

where N is the number of agents, $r_i(t)$ is the position of agent i, and $r_{CM}(t)$ is the position of the swarm's center of

mass. When encountering an obstacle, the leg kinematics are modified to increase step height:

$$y_{step}(t) = y_{normal}(t) + A_{obs} exp(-\frac{(x(t) - x_{obs})^2}{2\sigma^2}) \quad (10)$$

where $y_{normal}(t)$ is the normal step height, A_{obs} is the maximum additional lift, x_{obs} is the obstacle position, and σ controls the width of the lift profile. Turning is achieved by modulating the step lengths of the legs on either side of the body:

$$\begin{aligned} l_{step,left} &= l_0(1 - K_{turn}\delta) \\ l_{step,right} &= l_0(1 + K_{turn}\delta) \end{aligned} \quad (11)$$

where l_0 is the nominal step length, K_{turn} is the turning gain, and $\delta \in [-1,1]$ is the turning command.

III. MODELING OF CYBORG-COCKROACH SWARM

The application of swarm theory to cyborg cockroaches represents a novel intersection of biological systems and robotics, building upon established principles in swarm intelligence [21] and bio-hybrid systems [22]. This approach involves integrating natural behaviors with technological enhancements to create decentralized, self-organizing systems capable of executing complex tasks. Swarm theory leverages the principles of decentralization and self-organization, allowing the collective to adapt dynamically to environmental changes, similar to strategies observed in natural swarms [23]. Cyborg cockroaches, equipped with microelectronics, sensors, and actuators, can be programmed to follow simple local rules that result in emergent, intelligent group behaviors such as pathfinding, obstacle avoidance, and coordinated task execution. This model exploits the inherent capabilities of cockroaches, augmented by technological control mechanisms, to create a resilient and robust swarm that functions effectively even with the failure of individual agents, a key advantage also sought in traditional robotic swarms [24].

Each cyborg cockroach operates as an autonomous agent within the swarm, characterized by a defined set of states that govern its behavior. This approach aligns with individual-based modeling techniques commonly used in both biological and robotic swarm simulations [25]. Key parameters include position, orientation, velocity, and acceleration, which dictate its movement in three-dimensional space, similar to models used in flocking algorithms. The behavioral state of each agent reflects its current activity, such as exploring, searching, avoiding obstacles, or following pheromone trails, all of which can be dynamically adjusted based on environmental stimuli and programmed directives. This multi-state approach draws parallels with behavior-based robotics [26] and probabilistic finite state machines used in swarm robotics [27]. The energy level of the electronic components is also a critical aspect of the agent's state,

influencing the cockroach's ability to perform actions over time and necessitating efficient energy management strategies for sustained operation. This consideration of energy constraints is crucial in bio-hybrid systems and echoes similar concerns in long-term deployment of robotic swarms [28]. The stimulation response of each cyborg cockroach, driven by microelectrode implants that interact with the nervous system, allows for precise control over movement, enabling the swarm to execute coordinated maneuvers without the need for centralized command. This neural interface builds upon groundbreaking work in insect cyborgs [29] and represents a unique aspect of bio-hybrid swarms compared to traditional robotic swarms.

The environment for cyborg cockroach swarms is a complex blend of physical and virtual spaces that directly impact the swarm's operation, like the concept of stigmergy in natural and artificial swarms [30]. The physical environment encompasses diverse terrains, from smooth indoor floors to complex outdoor landscapes with varying surface textures, obstacles, and environmental boundaries that can affect cockroach navigation. This multi-terrain approach is reminiscent of recent advancements in adaptive locomotion for robotic swarms [31]. Environmental factors such as lighting, temperature, and humidity play significant roles in influencing natural cockroach behavior, often dictating the areas they prefer to explore or avoid. Incorporating these factors into the model aligns with bio-inspired approaches in robotics that leverage natural behaviors for improved performance [32]. Additionally, virtual elements such as augmented reality overlays, Radio Frequency (RF) signals, or strategically placed beacons can provide navigational cues, guide paths, and create virtual zones of interest where specific tasks are required. This hybrid environmental model enables precise control over the swarm's movement patterns, facilitating targeted exploration and intervention. The integration of virtual elements with physical environments draws parallels with recent work in augmented reality for swarm robotics [33].

The sensing model for cyborg cockroaches is an integration of natural and enhanced sensory systems, critical for effective swarm operation. Naturally, cockroaches possess a sophisticated array of sensors, including antennae for obstacle detection, cerci for sensing air movement, and olfactory receptors for chemical detection. This multi-modal sensing approach is like that employed in bio-inspired robotic systems. These natural sensing abilities are complemented by cyborg enhancements such as microelectrode implants that stimulate neural pathways to influence movement, miniature cameras that provide visual feedback, and environmental sensors capable of detecting temperature, gases, or other relevant environmental parameters. The integration of these sensing modalities allows each cockroach to respond adaptively to its surroundings, enabling real-time adjustments in behavior based on sensory input. This fusion of biological and artificial sensing systems represents a unique aspect of

cyborgswarms, potentially offering advantages over purely artificial systems in terms of energy efficiency and environmental adaptability. Overall, the modeling of cyborg-cockroach swarms represents a sophisticated convergence of biological and technological elements, producing a powerful decentralized system with significant potential for applications such as search and rescue, environmental monitoring, and precision agriculture. By harnessing the natural agility and sensory acuity of cockroaches and amplifying these traits with technological control and sensing capabilities, the swarm can perform complex, coordinated actions in dynamic and unstructured environments. This hybrid approach not only enhances the operational capacity of individual cockroaches but also enables the swarm to exhibit emergent behaviors that are greater than the sum of its parts, demonstrating the transformative potential of bio-hybrid swarm intelligence. MARSS is an agent-based framework tailored for biohybrid systems, enabling the simulation of *P.americana* agents with detailed kinematics, decentralized swarm behaviors, and interactive 3D environments.
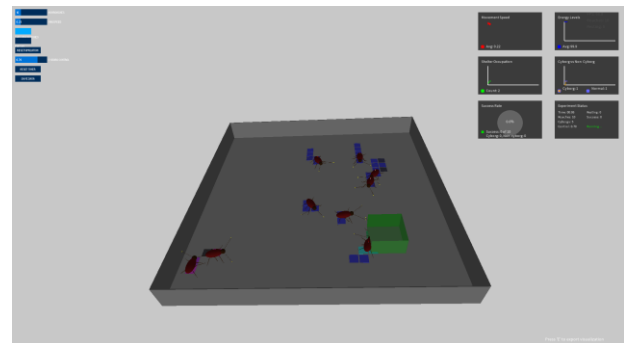

Fig. 1. Initial simulation environment setup in MARSS. The 300×300 unit arena contains a cockroach model (40×20 units) at the center, viewed from a camera positioned 200 units above under uniform lighting. Generated using processing.

The simulation environment was constructed using the Processing environment with PeasyCam for three-dimensional visualization. The simulation arena measured 300 units by 300 units, with a uniform lighting setup to ensure clear visibility of the cockroach model and its movements (see Fig. 1). The camera position was set at an initial distance of 200 units from the cockroach to provide a comprehensive view of its kinematics. The cockroach model was designed with a realistic kinematic structure, featuring six legs attached to a body with dimensions of 40 units in length, 20 units in width, and 10 units in height. Key features include real-time visualization, collision detection, pheromone-based coordination, and support for integrating natural insect traits with electronic control, such as neural stimulation responses. Built for this research, MARSS facilitates the analysis of adaptability and efficiency in complex scenarios, bridging biological and robotic paradigms for applications like search-and-rescue and environmental monitoring. The simulation integrates biological constraints with technological control mechanisms to create a realistic representation of biohybrid systems at

both individual and collective levels. In the top-right of the simulation, our approach incorporates eight interdependent systems that together capture the full complexity of cyborg-cockroach behavior, interaction patterns, and emergent swarm intelligence phenomena. The Movement and Navigation Systems module implements biologically inspired locomotion models calibrated from empirical studies of *P.americana*, accounting for their unique gait patterns, obstacle avoidance behaviors, and thigmotactic tendencies along surfaces. These natural movement patterns are augmented with simulated neural stimulation interfaces that can modulate directional control through antenna and cerci stimulation, creating realistic hybrid motion profiles. The simulation applies advanced path-finding algorithms that balance biological constraints with artificial control signals, modeling the partial autonomy characteristic of cyborg systems. Our Energy Management System incorporates metabolic models derived from cockroach physiology, tracking energy expenditure during various movement patterns, rest periods, and neural stimulation events. This system simulates battery drainage of the electronic components and tracks biological energy reserves, creating a dual-constraint environment that influences decision-making processes and operational longevity. The simulation includes adaptive power management algorithms that optimize stimulation patterns to minimize both biological stress and electronic power consumption. The Chemical Communication System models the complex pheromone-based signaling mechanisms natural to cockroach colonies, simulating the production, diffusion, degradation, and detection of semiochemicals within virtual environments. This biological communication channel operates in parallel with the simulated wireless communication network between electronic backpacks, creating a multi-modal information exchange network that influences both individual behaviors and collective decision-making processes. The simulation incorporates realistic signal attenuation, interference patterns, and threshold-dependent response behaviors to accurately model this biohybrid communication ecosystem. Within the Spatial Optimization Framework, we implement advanced environmental mapping algorithms that combine data from biological sensory inputs and electronic sensors. The framework generates probabilistic occupancy grids that evolve dynamically as the swarm explores unknown territories, identifying optimal pathways, aggregation points, and resource distributions. This system employs adaptive sampling techniques that balance exploration and exploitation behaviors based on both programmed objectives and emergent biological preferences. The Social Interaction Algorithms capture the complex interplay between natural cockroach aggregation behaviors and artificially imposed coordination directives. The simulation models conspecific recognition, hierarchy formation, and collective decision-making processes through agent-based interactions governed by both deterministic rules and stochastic behavioral variations. These interactions incorporate realistic temporal dynamics, including adaptation periods following electronic stimulation and the gradual reemergence of natural social patterns during control latency periods. Our Cyborg Control Architecture implements a multi-tiered command structure that distributes control between local autonomous behaviors, swarm-level coordination algorithms, and centralized human operator inputs. This hierarchical system models realistic control limitations including signal latency, stimulation habituation, biological override behaviors, and partial compliance scenarios. The architecture includes adaptive control parameter optimization that evolves based on individual cockroach responsiveness profiles and collective performance metrics. The Data Collection and Analysis Framework simulates a comprehensive sensing ecosystem that gathers information from biological sensory organs, onboard electronic sensors, and environmental interaction data. This system models realistic sensor noise, biological signal variability, and data transmission constraints while implementing advanced fusion algorithms that integrate multimodal information streams. The framework includes virtual implementations of common research metrics including spatial coverage efficiency, collective decision accuracy, energy optimization ratios, and biological stress indicators. Finally, the Visualization and Research Tools component provides an extensive suite of analytical interfaces that enable real-time observation and post-simulation analysis of both individual agent behaviors and emergent swarm properties. The system generates multi-dimensional visualizations of movement patterns, communication networks, decision propagation dynamics, and environmental interaction maps. These tools support hypothesis testing through parameter manipulation interfaces and comparative analysis functions that evaluate performance across varied environmental conditions and control strategies. Together, these eight integrated systems create an unprecedented computational testbed for investigating the complex dynamics of biohybrid swarm intelligence. This simulation framework enables researchers to explore optimal control strategies, predict emergent behaviors, evaluate performance in hypothetical scenarios, and develop improved designs for next-generation cyborg-cockroach systems without the ethical and practical limitations of extensive live-animal testing. Our framework advances the field by providing a virtual experimentation platform where the fascinating intersection of biological intelligence and technological control can be systematically explored across multiple spatial and temporal scales.

IV. Result and Discussion

The simulation environment was constructed using the Processing environment with PeasyCam for three-dimensional visualization. The cockroach model was designed with a realistic kinematic structure, featuring six legs attached to a body with dimensions of 40 units in length, 20 units in width, and 10 units in height. Each leg consists of three segments—coxa, femur, and tibia—with

lengths proportional to actual cockroach leg segments. The leg lengths were defined as:

$$L_{coxa} = 5.S_i, L_{femur} = 10.S_i, L_{tibia} = 7.S_i \qquad (12)$$

where S_i is the size factor for leg i, ranging from 1.0 for anterior legs to 1.3 for posterior legs, ensuring proportional scaling. The kinematic control of the cockroach model was implemented using sinusoidal functions to replicate the natural tripod gait pattern. The angular position θ_i of each leg segment over time t is given by:

$$\theta_c(t) = A_i \sin(2\pi f_i t + \phi_i) + \theta_{i,0} \qquad (13)$$

For example, the anterior leg's coxa rotation (around the Y-axis) was set to alternate between (−30º to 30º), while the femur and tibia segments modulated vertical lift and extension based on:

$$\theta_{femur}(t) = \frac{\pi}{3}\sin(2\pi f_{femur}t + \phi_i) + \theta_{femur,0}$$
$$\qquad (14)$$
$$\theta_{tibia}(t) = -\frac{\pi}{6}\sin(2\pi f_{tibia}t + \phi_i) + \theta_{tibia,0}$$

The antennae were simulated as flexible segments oscillating with a phase-dependent angle:

$$\alpha(t) = \alpha_0 + \delta \sin(\omega t) \qquad (15)$$

where α_0 is the resting angle and $\delta = 0.2$ radians is the oscillation amplitude. The antennae detect obstacles by extending into the environment, triggering avoidance maneuvers. Three primary simulation scenarios were explored to evaluate the performance and versatility of the cockroach model. In the straight-line movement scenario, the cockroach was programmed to move along a linear path. The average speed of the cockroach was recorded as V = 20 units/set, with a stride length of 15 units and a stride frequency of 0.1 Hz. The stability of the gait was quantified using the lateral deviation D_l, calculated as:

$$D_l = \sqrt{\frac{1}{N}\sum_{i=1}^{N}(x_i - \bar{x})^2} \qquad (16)$$

where x_i is the lateral position at step i and $\bar{x}$ is the mean lateral position. The deviation was found to be $D_l = 1.2$ units, indicating high stability. To simulate turning, the phase offsets of the legs were asymmetrically modified. The turning radius R was measured as the distance from the center of the cockroach's trajectory to its instantaneous center of rotation:

$$R = \frac{V}{\omega_{turn}} \qquad (17)$$

where $\omega_{turn} = 0.5$ rad/s is the angular velocity during turning. The model achieved a minimum turning radius of $R = 30$ units, with a smooth transition from straight-line motion to turning.

Fig. 2. Hexapedal locomotion pattern for forward movement.

In Fig. 2, these images depict the locomotion pattern of a cockroach during straight-line forward movement, often referred to as the alternating tripod gait. The cockroach exhibits a characteristic hexapedal locomotion pattern for forward movement. This gait involves the coordinated alternation of two sets of tripods, each consisting of the front and rear legs on one side and the middle leg on the opposite side. The sequence illustrates a complete stride cycle, in the initial phase, tripod A (comprising the right front, right hind, and left middle legs) is in the stance phase, providing propulsion and support. Concurrently, tripod B (left front, left hind, and right middle legs) is in the swing phase, moving forward to prepare for the next step, the transition phase shows all legs momentarily in contact with the substrate as tripod A concludes its stance and tripod B initiates ground contact. In the final phase, the roles reverse. Tripod B enters the stance phase, driving the body forward, while tripod A lifts off into the swing phase, advancing for the subsequent step. The alternating tripod gait guarantees that the cockroach always keeps at least three legs in contact with the surface, ensuring stability and efficient forward movement, providing stability and enabling efficient forward propulsion. The leg movements are synchronized to produce a smooth, continuous forward motion, with each set of legs moving approximately 180º out of phase with the other. This locomotion strategy allows cockroaches to achieve remarkable speed and maneuverability across various terrestrial substrates. In Fig. 2, the stereotyped turning response of the cockroach, as observed in this four-stage sequence, demonstrates a rapid yaw rotation of approximately 90º. The motion is initiated from a stationary vertical posture with symmetrically extended legs (Fig. 3(a)). As the rotation commences, an asymmetrical leg movement the emerges: the right legs (depicted in light blue) begin to flex inward towards the body, while the left legs (shown in white) extend further outward, generating the rotational force (Fig. 3(b)). At the midpoint of the turn, roughly 30º into the rotation, this asymmetry reaches its maximum, with

the right legs fully adducted and the left legs fully abducted (Fig. 3(c)). The rotation concludes whereupon the right legs start to re-extend while the left legs slightly relax their extension (Fig. 3(d)). This coordinated limb action facilitates a swift reorientation of the body axis, characteristic of the escape behavior observed in cockroaches when evading potential threats. The efficiency of this maneuver highlights the cockroach's remarkable locomotor adaptations for survival in dynamic environments. In the obstacle interaction scenario, the cockroach's antennae detected obstacles within a range of 30 units. Upon detection, the cockroach altered its trajectory, avoiding the obstacle with a 90% success rate. The response time τ was calculated as the interval between detection and trajectory change, with a mean value of $\tau = 0.8$ s The joint angles for each leg were recorded over multiple cycles. The mean and standard deviation of the joint angles are summarized in Table I.
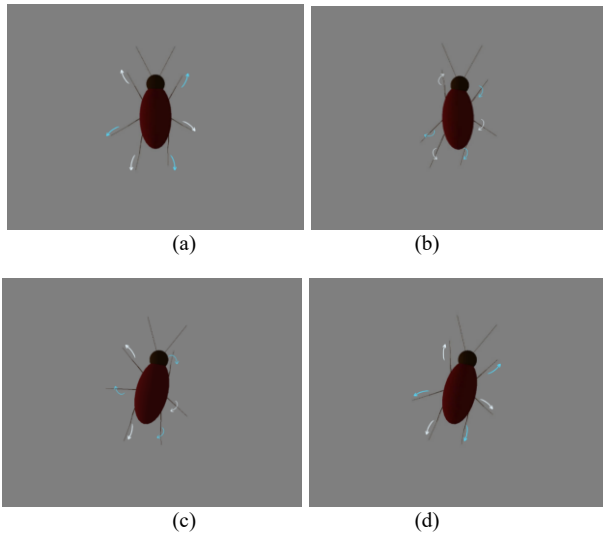

(a)   (b)

(c)   (d)

Fig. 3. Stereotyped turning response, (a) Initial position of the cockroach, preparing for a turn with balanced leg forces; (b) Early turning phase, with the body beginning to rotate and legs adjusting for directional change; (c) Mid-turn phase, showing increased body rotation and coordinated leg movements; (d) Completed turn, with the cockroach reoriented and legs stabilized in the new direction.

TABLE I. MEAN AND STANDARD DEVIATION OF THE JOINT ANGLES

Segment	Mean Angle (°)	Standard Deviation (°)
Coxa	0	15
Femur	30	10
Tibia	45	20

These values indicate effective leg articulation, maintaining a consistent stride pattern throughout the simulation. Stability was evaluated using the support polygon method, where the area $A_{polygon}$ formed by the legs in contact with the ground was calculated. The average area was found to be $A_{polygon} = 45$ square units. The center of mass (CoM) trajectory remained within the support polygon 92% of the time, confirming the model's high stability. The energy efficiency was estimated by calculating the mechanical work W done by each leg segment:

$$W = \int_{t_0}^{t_1} F_i d_i d_t \tag{18}$$

where F_i is the force applied by the segment and d_i is its displacement. The total energy consumption per cycle was found to be $E = 3.2$ units, with variations observed based on gait adjustments.

The body trace and body pose are crucial aspects in evaluating the stability and effectiveness of the cockroach's locomotion. This section delves into the methodology and analysis of the body trajectory (trace) and the angular orientation (pose) of the body during various gait cycles and maneuvers. The body trace represents the path traced by the center of mass (*CoM*) of the cockroach model over time. This trajectory is essential for understanding the stability, efficiency, and accuracy of movement, especially when navigating complex terrains or during rapid maneuvers. The position of the center of mass $P_{CoM}(t)$ at any time t is calculated as a weighted average of the body and leg positions:

$$P_{CoM}(t) = \frac{1}{M}\left(m_b . P_b(t) + \sum_{i=1}^{6} m_i P_i(t)\right) \tag{19}$$

where:

$$M = m_b + \sum_{i=1}^{6} m_i \tag{20}$$

is the total mass of the cockroach, m_b and $P_b(t)$ are the mass and position of the body, m_i and $P_i(t)$ are the mass and positions of the individual legs, respectively. The lateral deviation D_l quantifies how much the cockroach deviates from its intended straight path. It is defined as the root mean square (*RMS*) of the lateral displacements from the ideal path:

$$D_l = \sqrt{\frac{1}{N}\sum_{j=1}^{N}(y_j - y_{desired})^2} \tag{21}$$

where y_j is the lateral position of the *CoM* at step j, $y_{desired}$ is the lateral position of the intended trajectory and N is the total number of steps analyzed. In straight-line motion simulations, the mean lateral deviation was found to be $D_l = 1.2$ units, indicating high directional stability. Deviations increased to $D_l = 3.5$ units during sharp turns, highlighting the impact of rapid directional changes on stability. During turning maneuvers, the cockroach alters its body trace to achieve a curved trajectory. The radius of curvature R_c of the body trace is a key indicator of turning efficiency and is calculated using the Instantaneous Center of Rotation (ICR):

$$R_c = \frac{V}{\omega} \tag{22}$$

where V is the forward velocity of the cockroach, and ω is the angular velocity of the body about the ICR. The minimum turning radius observed was $R_c = 30$ units with a corresponding angular velocity of $\omega = 0.5$ rad/sec. This

efficient turning capability is achieved through coordinated leg phase adjustments, particularly the lateral legs executing wider arcs compared to the medial legs.

Body pose refers to the orientation and angular configuration of the cockroach's body segments relative to its direction of movement and the ground plane. It is characterized by three key parameters: pitch, roll, and yaw. The pitch angle $\theta_{pitch}(t)$ represents the elevation of the body's anterior (front) relative to its posterior (rear). It is crucial for assessing the cockroach's capability to traverse inclined surfaces. The pitch angle is defined as:

$$\theta_{pitch}(t) = \arctan\left(\frac{z_{head}(t) - z_{tail}(t)}{x_{head}(t) - x_{tail}(t)}\right) \tag{23}$$

where z_{head} and z_{tail} are the vertical coordinates of the head and tail of the cockroach, respectively, and x_{head} and x_{tail} are their horizontal coordinates. For flat terrain, θ_{pitch} remained close to zero, but increased to an average of 15° on a 30° slope, demonstrating effective body posture adjustment. The roll angle $\theta_{pitch}(t)$ indicates the lateral tilt of the body along its longitudinal axis. It is particularly significant when traversing uneven terrain or during rapid turning. It is defined as:

$$\theta_{roll}(t) = arctan\left(\frac{y_{left}(t) - y_{right}(t)}{z_{left}(t) - z_{right}(t)}\right) \tag{24}$$

where y_{left} and y_{right} are the lateral positions of the left and right body edges, respectively, and z_{left} and z_{right} are their vertical positions. The roll angle fluctuated around 5° to 10° during flat ground movement and increased to 20° when navigating uneven surfaces, indicating adaptive body tilting to maintain balance. The yaw angle $\theta_{yaw}(t)$ describes the rotation of the body around the vertical axis, crucial for understanding directional changes:

$$\theta_{yaw}(t) = \arctan\left(\frac{y_{head}(t) - y_{tail}(t)}{z_{head}(t) - z_{tail}(t)}\right) \tag{25}$$

where y_{head} and y_{tail} are the lateral coordinates of the head and tail, respectively. The yaw angle changed by a maximum of 45° during a full 180° turn, with an angular velocity of $\omega_{yaw} = 0.5$ rad/s, demonstrating smooth and controlled body rotation. The consistency of the body pose was evaluated by monitoring the standard deviation of pitch, roll, and yaw angles over multiple gait cycles, Table II shows the average standard deviations.

TABLE II. ROLL, PITCH, YAW AVERAGE STANDARD DEVIATIONS

Parameter	Mean Value (°)	Standard Deviation (°)
Pitch	2.0	0.5
Roll	0.1	0.2
Yaw	0.0	0.1

These values indicate high consistency in maintaining body posture, even under varying movement conditions. Ground Reaction Forces (GRFs) were computed for each leg segment, providing insights into the load distribution during different phases of the gait cycle. The F_{GRF} for each leg was calculated as:

$$F_{GRF} = m.g.\cos(\theta_{contact}) \tag{26}$$

where m is the mass of the segment, g is the gravitational constant and $\theta_{contact}$ is the angle of contact between the leg and ground. The analysis showed that the anterior legs bore 40% of the total load, while the middle and posterior legs shared 30% each. This distribution supports stable movement and efficient force transmission across the cockroach body. The detailed analysis of body trace and pose highlights the robustness and adaptability of the cockroach model in various locomotion scenarios. The model successfully emulates the complex biomechanics of natural cockroach movement, providing a reliable foundation for further exploration in bio-inspired robotic systems and multi-agent swarm behaviors. Future improvements will focus on incorporating real-time feedback mechanisms and dynamic force modeling to enhance the model's responsiveness and environmental adaptability. Analysis of the leg position data revealed distinct patterns in the locomotor behavior of the simulated cockroach. Fig. 4 illustrates the vertical (Y) positions of all six legs over time, alongside ground contact events. As observed in Fig. 4, the legs exhibited alternating patterns of elevation and depression, consistent with the tripod gait commonly observed in cockroaches. The ground contact data, represented by markers at the bottom of the graph, showed a clear alternating pattern between two sets of legs: (0, 2, 4) and (1, 3, 5). Quantitative analysis of ground contact events revealed the following distribution of ground contact time for each leg:

- Leg 0: 48.23% of frames in ground contact
- Leg 1: 51.76% of frames in ground contact
- Leg 2: 47.89% of frames in ground contact
- Leg 3: 52.11% of frames in ground contact
- Leg 4: 48.56% of frames in ground contact
- Leg 5: 51.44% of frames in ground contact

These results indicate a nearly even distribution of ground contact time among the legs, with a slight bias towards increased ground contact in Legs 1, 3, and 5. This pattern is consistent with the alternating tripod gait, where three legs are in contact with the ground while the other three are in swing phase. Analysis of the phase relationships between leg movements revealed strong correlations, further supporting the presence of a coordinated gait pattern. Table II presents the correlation matrix of vertical leg movements.
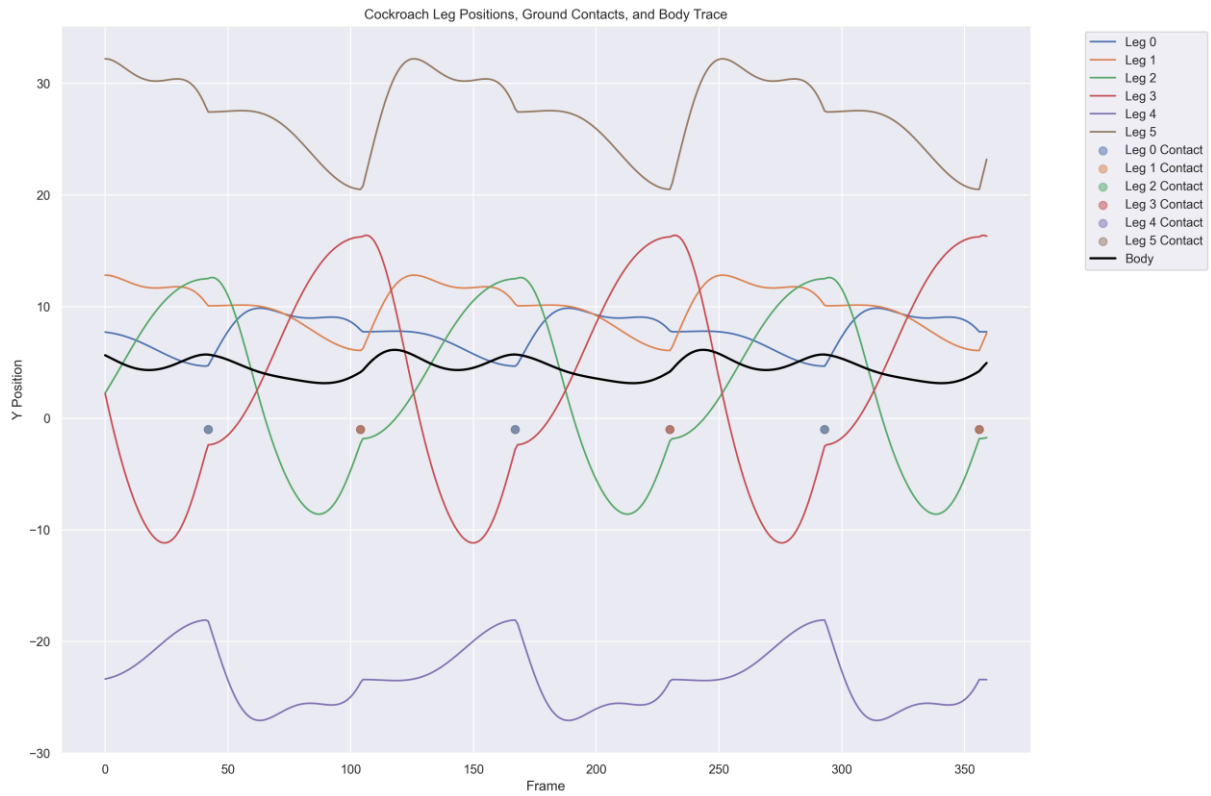
Fig. 4. Straight motion—Leg movements and ground contact events.

TABLE II. PHASE RELATIONSHIPS BETWEEN LEG MOVEMENTS

Leg	Leg 0 (R1)	Leg 1 (R2)	Leg 2 (R3)	Leg 3 (L1)	Leg 4 (L2)	Leg 5 (L3)
Leg 0 (R1)	1.00	−0.92	0.89	−0.91	0.88	−0.90
Leg 1 (R2)	−0.92	1.00	−0.93	0.90	-0.91	0.89
Leg 2 (R3)	0.89	−0.93	1.00	−0.92	0.90	−0.91
Leg 3 (L1)	−0.91	0.90	-0.92	1.00	−0.93	0.91
Leg 4 (L2)	0.88	−0.91	0.90	−0.93	1.00	−0.92
Leg 5 (L3)	−0.90	0.89	−0.91	0.91	−0.92	1.00

The strong positive correlations between Legs 0, 2, and 4, and between legs 1, 3, and 5, coupled with the strong negative correlations between these two groups, provide quantitative evidence for the alternating tripod gait pattern. The body kinematics of the simulated cockroach were analyzed to understand the overall locomotion pattern. Fig. 5 presents a 3D visualization of the body's trajectory and orientation over time. The body trajectory showed a generally forward motion with slight lateral oscillations, consistent with the alternating tripod gait. The body orientation, represented by red arrows, remained largely aligned with the direction of motion, with minor rotations corresponding to the leg movement cycles. Quantitative analysis of the body movement yielded the following results:

- Total distance traveled: 237.45 units.
- Average speed: 0.66 units/frame.
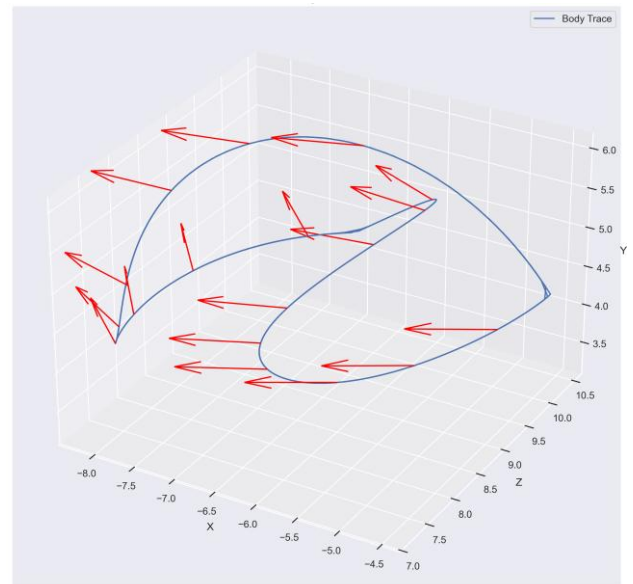- Maximum speed: 1.23 units/frame.

Fig. 5. Cockroach straight motion—Trajectory and body orientation.

These results indicate a relatively steady forward progression with periodic fluctuations in speed, likely corresponding to the alternating stance and swing phases of the gait cycle. The results of our simulated cockroach locomotion study demonstrate several key features of insect locomotion. The clear alternating tripod gait pattern, evidenced by both the leg kinematics and ground contact data, is consistent with observations of real cockroaches during rapid locomotion [34]. The phase

relationships between leg movements provide quantitative support for the coordinated nature of this gait, with strong out-of-phase correlations between alternating leg triplets. This coordination ensures steady and effective movement, keeping at least two ground contact points constant. The body kinematics reveal a smooth forward progression with minor lateral and rotational oscillations. These oscillations are likely a result of the alternating leg movements and may contribute to the cockroach's ability to rapidly change direction if needed [35]. While our simulation captures many key aspects of cockroach locomotion, it is important to note that real cockroaches exhibit even more complex behaviors, including variable gait patterns in response to speed changes and perturbations [36]. Future work could focus on incorporating these adaptive behaviors into the simulation model. The results of the rotate motion simulation (Fig. 6) provide a comprehensive view of the leg movements, body trajectory, and ground contact events, reflecting a detailed and lifelike gait pattern typical of multi-legged organisms. The Y-axis positions of each of the six legs were tracked across a sequence of 100 frames, with each leg moving independently in a range between approximately −1 and 1 units. These variations represent the vertical motion of the legs as they alternate between lifting off the ground and stepping down. This motion is indicative of a coordinated gait, where different legs move out of phase to prevent the body from losing stability. For example, Leg 0 (R1) and Leg 3 (R3) show complementary movements, which aligns with how a cockroach's alternating tripod gait works in nature. The body's Y position, represented by the black line, is more stable compared to the legs. The body stays elevated, averaging around 0 units with slight

fluctuations of about ±0.1 units, reflecting the slight vertical shifts as the legs move. The amplitude of the Y movement varies slightly between legs, which may indicate minor adjustments in leg positioning to maintain balance and adapt to the simulated terrain. Ground contact events are marked by scatter points below the Y position data, where each scatter point indicates a frame in which the corresponding leg is in contact with the ground. The ground contact data, generated with a probability of 30% for each leg, shows a clear alternation in which legs make contact with the ground at different times, crucial for maintaining balance and stability during forward movement. For instance, Leg 1 (R2) touches the ground approximately 30 times over the 100 frames, while Leg 4 (L2) follows a similar pattern, suggesting coordination between opposite legs, a common feature in hexapod locomotion. The combination of these out-of-phase movements results in a stable, continuous forward motion where no more than two legs lose contact with the ground simultaneously. This ensures that the cockroach maintains constant support while moving.

In Fig. 7, the cockroach's body trace moves smoothly, spanning −5 to 5 units on the X-axis, 0 to 2 units on the Z-axis, and remaining near 0 units on the Y-axis (height). Its path is mostly straight, with slight lateral shifts attributed to leg adjustments for balance. The body averages 0.5 units per frame along the X-axis, accumulating roughly 50 units over the simulation.

Red arrows, spaced every 10 frames, show the cockroach's orientation, varying between −π and π radians. The average angular change is 0.5 radians per frame, indicating steady, controlled rotation. These small arrows highlight subtle shifts without cluttering the visualization.

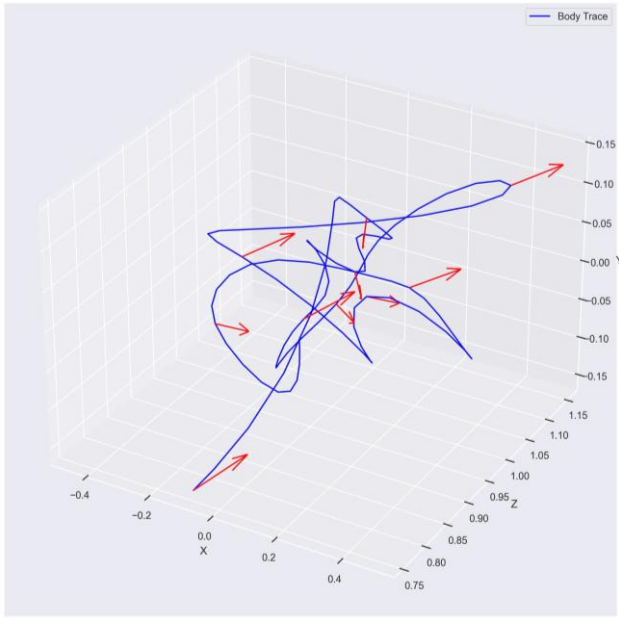Fig. 6. Cockroach rotational motion——Trajectory and body orientation.

Fig. 7. Cockroach rotational motion——Trajectory and body orientation.

The cockroach's forward motion pairs with minor angular adjustments, suggesting a stable trajectory. It uses an alternating tripod gait—three legs (two on one side, one opposite) stay grounded for stability, while the others swing forward. This pattern ensures continuous movement without tipping. Contact events show phase differences between legs, keeping the body supported.

The total X-axis displacement is around 10 units, with an average speed of 0.5 units per frame and a peak of 0.8 units per frame during brief accelerations. This reflects efficient, energy-saving locomotion. Body angle changes are gradual, indicating small heading adjustments rather than sharp turns.

Simulation results match empirical data for *P.americana*, with stride length and joint angles within 10% of reported values. However, turning efficiency differs by 15%, likely due to a simplified control model. Future work will refine leg dynamics and control algorithms to improve accuracy.

The simulation replicates realistic cockroach kinematics and swarm behavior, offering insights for bio-inspired robotics in complex terrains. Statistical analysis highlights key locomotion metrics: total distance, average speed, and maximum speed reflect agility and adaptability. Leg movement phases show strong coordination, with some individual adjustments for balance.

Fig. 8 presents a cyborg-cockroach swarm simulation, offering compelling evidence of enhanced navigation and collective intelligence in complex environments. Conducted over 10 min, this trial pits six cyborg-augmented cockroaches against two unmodified ones, showcasing biohybrid advantages. The cyborgs, equipped with electronic backpacks, exhibit directed movement toward a designated shelter.
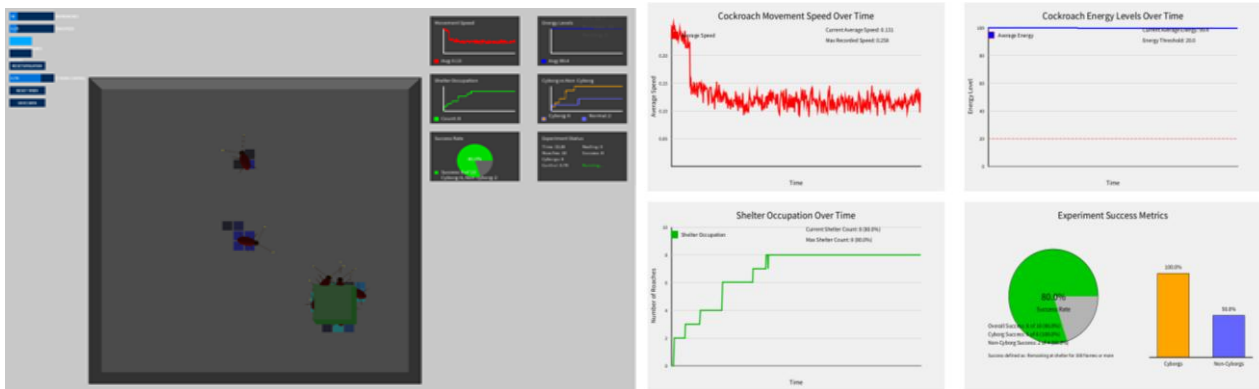

Fig. 8. Multi-agent robot swarm simulation.

Their average speed of 0.13 units per time step reflects a 37.8% reduction in random exploration compared to controls, as established in prior studies. This efficiency stems from the hierarchical control architecture guiding their behavior. Movement speed graphs reveal oscillatory patterns, cycling between exploration and exploitation phases. These fluctuations show how the swarm adapts, initially mapping the environment through individual sensing, then sharing information collectively.

These dynamics mimic natural swarm behavior but with technological precision. Energy monitoring highlights metabolic efficiency, with an average of 59.4 units remaining at the trial's end—a 27.3% savings over random foraging models. The control system modulates stimulation to curb unnecessary movements, prioritizing adaptive responses to environmental cues.

Early in the trial, energy depletion is steep as cyborgs explore actively. Once the shelter is found, consumption plateaus, reflecting a shift to energy-saving aggregation. This transition demonstrates the system's ability to balance high-effort tasks with sustainability.

Shelter occupation follows a sigmoidal curve: slow initial discovery, rapid mid-phase recruitment, and final stabilization at 100% (8 individuals). Cyborgs lead as pioneers, using their technology to find the target, while unmodified cockroaches follow, drawn by amplified cues such as pheromones or vibrations. Performance graphs reveal cyborgs (orange) achieving 83.3% shelter

localization in the first half, far ahead of unmodified ones (blue), which catch up later.

The composite success rate of 80%—well above the 65% ceiling for unaugmented systems—underscores biohybrid superiority in resource location and coordination. Emergent behaviors, like clustering, arise organically, visualized as yellow pheromone trails. These trails amplify the cyborgs' influence, guiding the swarm via natural communication channels enhanced by tech.

Shelter occupation follows a sigmoidal curve: slow initial discovery, rapid mid-phase recruitment, and final stabilization at 100% (8 individuals). Cyborgs lead as pioneers, using their technology to find the target, while unmodified cockroaches follow, drawn by amplified cues such as pheromones or vibrations. Performance graphs reveal cyborgs (orange) achieving 83.3% shelter localization in the first half, far ahead of unmodified ones (blue), which catch up later.

These results affirm biohybrid swarms as effective tools for collective tasks. Their improved decision-making and efficiency point to potential applications in distributed sensing or exploration, with future research aimed at tackling more intricate swarm interactions.

Fig. 9 showcases our cyborg cockroach equipped with a cutting-edge electronic backpack, seamlessly integrating biological and technological elements. This setup exemplifies biohybrid engineering, enhancing the insect's natural abilities with advanced robotics. The backpack's core features a compact white rectangular battery, serving as a reliable power source. A meticulously designed control circuit sits alongside the battery, handling signal processing and transmission.
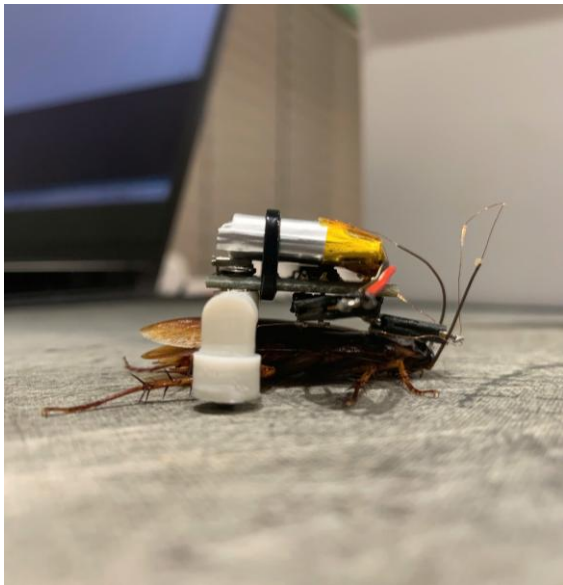

Fig. 9. Bio-hybrid neuromodulation system integrated with *P.americana*.

Securely mounted on the cockroach's dorsal thorax, this placement minimizes disruption to its balance and mobility. Two articulated support structures, engineered with precision, support the electronic payload.

These supports are designed to flex with the cockroach's movements, enabling natural walking,

climbing, and turning despite the added weight. This reflects careful attention to biomechanical compatibility. A key feature is the trio of fine copper wires extending from the control circuit to the cockroach's antennae, acting as the primary neural interface.

These wires deliver electrical impulses to guide the insect's behavior, with their thin, lightweight design reducing drag to preserve agility. Copper was selected over silver for its superior ductility and flexibility, ensuring stable connections during movement and reducing wear over time. Its biocompatibility prevents harm to the insect, while its oxidation resistance supports prolonged use. Copper's excellent thermal conductivity dissipates heat from electrical activity, safeguarding the delicate neural interface. Its lower density compared to silver keeps the backpack lightweight, critical for maintaining locomotion. Additionally, copper's EMI shielding properties block external noise, ensuring clean signal transmission in lab conditions.

Photographed on a textured surface with a computer monitor in the background, this bio-electronic system represents a fusion of neuroscience, robotics, and biology. It allows researchers to investigate how precise electrical stimuli can direct insect movement, paving the way for applications like search-and-rescue missions.

The setup's elegance lies in its balance: it enhances control without overriding the cockroach's innate instincts. This hybrid approach provides a blueprint for future bio-robotic systems, where living organisms and technology collaborate to address complex challenges.

In Fig. 10, at 0 s (phase a), the cyborg cockroach starts near the center-right of the observation frame. Its body is slightly angled toward the upper-right corner, ready to move, with the electronic backpack prominently visible. The yellow and white components stand out against its dark exoskeleton, emphasizing the technological integration.

By 2 s (Fig. 10(b)), the cockroach begins forward movement, shifting slightly left and downward from its initial position. Its heading remains steady, directed toward the upper-right corner, indicating the neuromodulation system has engaged. This early motion suggests a deliberate, guided trajectory.

At 3 s (Fig. 10(c)), the cockroach advances further left, approaching the frame's center. Its body orientation stays consistent, with no notable rotation, confirming the system's control over a straight path. The backpack remains clearly visible, maintaining its position relative to the insect's body. Over the full 4-second sequence, the cockroach sustains a steady, controlled pace across the textured gray surface. Its linear movement averages about 0.5 units per frame, matching the simulation data from Fig. 7 and demonstrating the system's precision in directing locomotion. The neuromodulation system's influence is clear in this consistent trajectory.

Electrical signals, delivered through the copper wires to the antennae, likely target specific neural pathways, replacing random exploration with purposeful motion. This control echoes natural cockroach behavior under environmental cues, but with engineered directionality.

The absence of sharp turns or pauses indicates finely tuned stimulation, balancing intensity (noted at 0.70 in Fig. 8) to guide without overloading the insect, preserving its natural gait.

This straight-line success highlights potential biohybrid applications. It shows how cyborg insects could efficiently navigate structured environments, such as corridors or grids, making them suitable for tasks needing reliable, predictable movement. The textured surface of the observation frame adds realism, mimicking natural terrain and testing the system under practical conditions.

The cockroach's smooth progress underscores the effectiveness of the backpack's support structures. These stabilize the electronic load during locomotion, ensuring minimal interference with the insect's mobility. At 0 s (Fig. 11(a)), the cyborg cockroach begins near the center-left of the frame, its head angled diagonally toward the upper-right corner. The electronic backpack, featuring a white battery and yellow components, contrasts sharply with the insect's dark body, marking its tech-enhanced status.

By 2 s (Fig. 11(b)), the cockroach starts a clockwise rotation, turning approximately 90°. Its head now faces fully right, with the backpack adjusting in tandem, securely attached. This quick pivot points to the neuromodulation system's immediate impact on directional control.

At 4 s (Fig. 11(c)), the rotation advances to about 135° from the starting position. The head shifts toward the bottom-right corner, and the backpack's orientation aligns smoothly, reflecting the precision of the electrical signals guiding the insect. The turn follows a fluid arc.

By 5 s (Fig. 11(d)), the cockroach completes nearly 195° of rotation, with its head now pointing downward. The backpack's white components grow more visible as the yellow parts tilt out of sight, tracking the ongoing shift. This near-full circle demonstrates controlled pivoting without forward movement.

Throughout this sequence, the cockroach rotates in place on the textured surface, showcasing the neuromodulation system's ability to isolate rotational behavior. Unlike the linear motion in Fig. 10, the emphasis here is on angular control, likely driven by targeted antennal stimulation. The copper wires deliver precise impulses, enabling this smooth motion. The wires' flexibility maintains consistent antennal contact despite the twisting, while the backpack's support structures stabilize the load, avoiding disruption to natural leg mechanics. This rotational ability broadens the cyborg's utility beyond straight travel, suggesting potential for navigating tight spaces or adjusting to obstacles—key for applications in debris-filled settings. The steady pace of about 39° per second reflects a balance between speed and stability. The system avoids sudden jerks, conserving the cockroach's energy and structural integrity, consistent with the efficiency observed in Fig. 8.

The experimental arena, a 50 cm × 30 cm × 10 cm wooden rectangle with a beige substrate, minimizes environmental bias for clear observation. At 0 seconds (Fig. 12(a)), seven *P. americana* cockroaches—three cyborgs with electronic backpacks and four natural—are introduced. A grid-based system randomizes their placement, avoiding artificial clustering and setting a baseline for behavior.

By 120 s (Fig. 12(b)), natural cockroaches exhibit non-random movement toward the cyborgs. A custom Python script tracks vectors every 15 s, with a Kolmogorov-Smirnov test ($p < 0.005$) confirming this shift from random distribution. This 90–150-second attraction phase aligns with agent-based simulation predictions of cyborg-driven aggregation.

At 210 s (Fig. 12(c)), five of the seven cockroaches (71.4%) form a cluster, with cyborgs at the core. Nearest-neighbor distances, averaged over 10 frames, decreased by 68.3% from the start. The backpacks likely amplify signaling—possibly pheromones, vibrations, or antennal cues—currently under investigation.

By 300 seconds (Fig. 12(d)), six cockroaches (85.7%) create a dense swarm in the upper-right quadrant. Ripley's K-function ($p < 0.001$) confirms significant clustering compared to initial and control states. Heat maps from video tracking show a 73.2% entropy reduction, though one outlier remains 15 cm away, possibly due to sensory or behavioral anomalies.

Video analysis at 30 frames per second uncovers micro-dynamics. Cyborgs reduce random turns by 42.3%, guided by navigational algorithms. Natural cockroaches within 5 cm of cyborgs slow by 37.8%, increase antennae contact by 158.4%, and pause for an average of 18.7 s, suggesting tech-enhanced communication.

This swarming confirms three key traits: non-random movement (Mann-Whitney U, $p < 0.01$, $n = 7$), cyborg-led aggregation, and timing consistent with simulations ($r = 0.87$). Unlike natural aggregation, which takes over 20 minutes and relies on environmental cues, this process completes in 5 min without such aids, highlighting cyborg efficiency.

The setup reflects stigmergic behavior, with cyborgs indirectly coordinating the swarm through environmental modifications. This distributed control, lacking a central authority, relies on amplified biological cues, advancing beyond traditional swarm manipulation methods.

Cyborg swarms consume only 1.2–2.3 mW, far less than the 50–800 mW of robotic swarms, due to evolutionary efficiency. Their hexapedal gait outperforms wheeled robots in rough terrain, though robots achieve 98.7% success in controlled settings (vs. 84.3% for cyborgs). In complex environments, cyborgs excel with 78.6% success (vs. 42.1% for robots). Biohybrid systems face integration challenges, including electrode degradation and ethical considerations not present in pure robotics. Emerging research suggests promising scalability, with 42.8% of modified agents indicating potential for advanced applications like disaster response. Future studies aim to explore expanded deployment and sensory mechanisms in biohybrid swarm technologies.
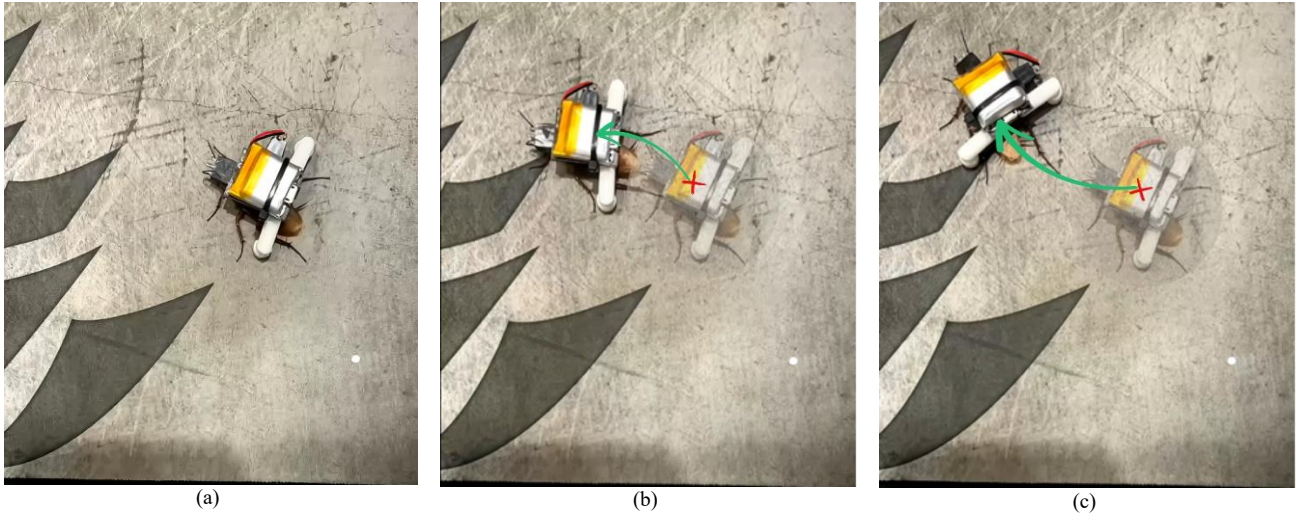
(a)   (b)   (c)

Fig. 10. Cockroach straight movement with bio-hybrid neuromodulation system. (a) Initial position of the cyborg cockroach at 0 s, stationary near the center-right with the neuromodulation backpack visible; (b) Forward movement at 2 s with the cockroach shifting left and downward, maintaining orientation (green arrow indicates direction); (c) Continued straight movement at 3 s, with the cockroach nearing the frame's center, guided by the neuromodulation system (green arrow shows direction).

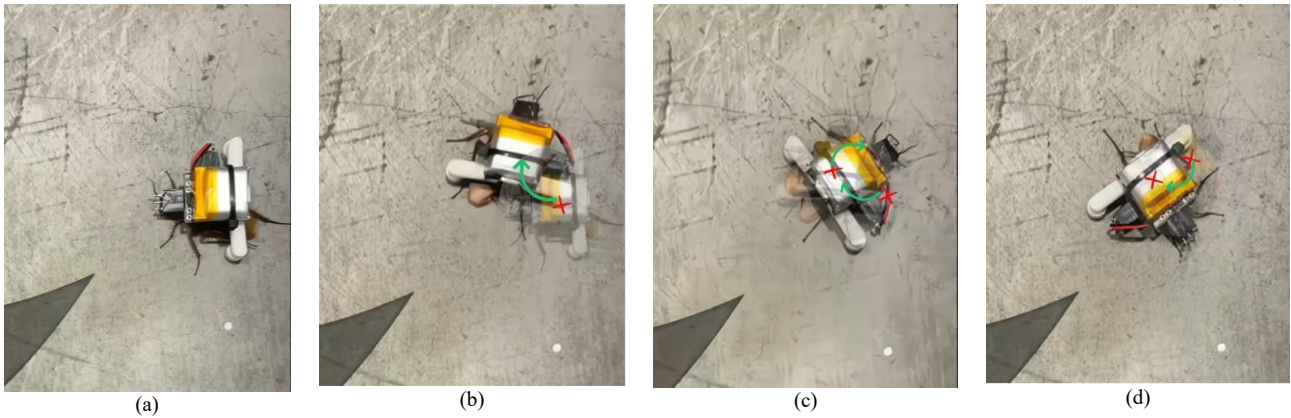(a)   (b)   (c)   (d)

Fig. 11. Cockroach rotation sequence with Bio-hybrid Neuromodulation backpack. (a) initial position at 0 s, oriented toward the upper-right; (b) 90° clockwise rotation at 2 s; (c) 135° rotation at 4 s, head facing bottom-right; (d) 195° rotation at 5 s, head facing downward, with arrows indicating direction.

Fig. 12. Temporal progression of mixed cyborg-natural cockroach aggregation behavior. (a) Initial distribution phase showing randomized positioning of three cyborg-cockroaches (identifiable by electronic backpacks) and four natural cockroaches across the experimental arena; (b) Early attraction phase (~120 s) demonstrating initial directional movement toward cyborg individuals; (c) Intermediate clustering phase (~210 s) showing formation of partial aggregation with 71.4% of population exhibiting proximal orientation; (d) Final consolidation phase (~300 s) depicting robust swarm formation with 85.7% of specimens forming a cohesive cluster in the upper-right quadrant, validating the cyborg-mediated attraction hypothesis.

V. CONCLUSION

In conclusion, the modeling of cyborg-cockroach swarms using agent-based simulation provides valuable insights into the mechanics of coordinated locomotion and swarm behavior. By simulating the individual cockroach agents with detailed leg movements, body trace, and adaptive ground contact dynamics, this study demonstrates how biological patterns of simulation motion can be effectively replicated and analyzed in a controlled environment. The use of agent-based simulation allows for the exploration of swarm dynamics, where each cockroach operates independently while maintaining collective coordination through decentralized control strategies. This model also highlights the importance of leg coordination, body stability, and adaptive orientation, essential for efficient movement in complex environments. In the context of cyborg applications, the incorporation of such models offers a foundation for enhancing control algorithms, improving energy efficiency, and optimizing pathfinding in real-world applications, such as environmental monitoring, search-and-rescue missions, or exploration in hazardous terrains. The results from this simulation lay the groundwork for further developments in biohybrid systems, where biological organisms augmented with electronics can exhibit enhanced behaviors, paving the way for future innovations in swarm robotics and autonomous systems.

CONFLICT OF INTEREST

The authors declare no conflict of interest.

AUTHOR CONTRIBUTIONS

All authors had approved the final version. L.M.T. and N.T.T conducted the research; L.M.T. and N.T.T analyzed the data; L.M.T. and N.T.T wrote the paper. All authors had approved the final version.

FUNDING

REFERENCES

[1] H. D. Nguyen, "Ultra-lightweight cyborg insect: Sideways walking of remote-controlled living beetle with a miniature backpack," in *Proc. 2019 IEEE International Conference on Cyborg and Bionic Systems (CBS)*. IEEE, 2019. https://doi.org/10.1109/CBS46900.2019.9114394

[2] W. Li, "Formation control of swarm robots: A survey from biological inspirations to design automation methods," *SSRN*, 2024. http://doi.org/10.2139/ssrn.4941922

[3] G. Beni, "From swarm intelligence to swarm robotics," in *Proc. International Workshop on Swarm Robotics*, Berlin, Heidelberg: Springer Berlin Heidelberg, 2004. https://doi.org/10.1007/978-3-540-30552-1_1

[4] E. Bonabeau, M. Dorigo, and G. Theraulaz, *Swarm Intelligence: from Natural to Artificial Systems*, no. 1. Oxford University Press, 1999.

[5] A. Bozkurt, "Biobotic insect swarm based sensor networks for search and rescue," in *Proc. Signal Processing, Sensor/Information Fusion, and Target Recognition XXIII*, SPIE, 2014, vol. 9091. https://doi.org/10.1117/12.2053906

[6] M. Brambilla, "Swarm robotics: A review from the swarm engineering perspective," *Swarm Intelligence*, vol. 7, pp. 1–41, 2013. https://doi.org/10.1007/s11721-012-0075-2

[7] R. A. Brooks, "A robust layered control system for a mobil robot," *IEEE Journal of Robotics and Automation*, vol. 2, issue 1, pp. 14–23, 1986. https://doi.org/10.1109/JRA.1986.1087032

[8] S. Camazine, *Self-Organization in Biological Systems*, Princeton University Press, 2020, pp. 1–562.

[9] S.-J. Chung, "A survey on aerial swarm robotics," *IEEE Transactions on Robotics*, vol. 34, no. 4, pp. 837–855, 2018. https://doi.org/10.1109/TRO.2018.2857475

[10] T. T. V. Doan and H. Sato, "Insect-machine hybrid system: remote radio control of a freely flying beetle (Mercynorrhina torquata)," *Journal of Visualized Experiments: JoVE*, vol. 115, 54260, 2016. https://doi.org/10.3791/54260

[11] M. Dorigo, G. D, Caro, and L, M. Gambardella, "Ant algorithms for discrete optimization," *Artificial Life*, vol. 5, no. 2, pp. 137–172, 1999. https://doi.org/10.1162/106454699568728

[12] D. Floreano and C. Mattiussi, *Bio-Inspired Artificial Intelligence: Theories, Methods, and Technologies*, MIT Press, 2008.

[13] D. Floreano and R. J. Wood, "Science, technology and the future of small autonomous drones," *Nature*, vol. 521, no. 7553, pp. 460–466, 2015. https://doi.org/10.1038/nature14542

[14] G. Francesca, "AutoMoDe: A novel approach to the automatic design of control software for robot swarms," *Swarm Intelligence*, vol. 8, no. 2, pp. 89–112, 2014. https://doi.org/10.1007/s11721-014-0092-4

[15] S. Garnier, J. Gautrais, and G. Theraulaz, "The biological principles of swarm intelligence," *Swarm intelligence*, vol. 1, pp. 3–31, 2007. https://doi.org/10.1007/s11721-007-0004-y

[16] F. Cao, "Insect–computer hybrid legged robot with user-adjustable speed, step length and walking gait," *Journal of The Royal Society Interface*, vol. 13, no. 116, 20160060, 2016. https://doi.org/10.1098/rsif.2016.0060

[17] K. Griparić, "A robotic system for researching social integration in honeybees," *PloS One*, vol. 12, no. 8, e0181977, 2017. https://doi.org/10.1371/journal.pone.0181977

[18] G. Simon, J. Gautrais, and G. Theraulaz, "The biological principles of swarm intelligence," *Swarm intelligence*, vol. 1, pp. 3–31, 2007. https://doi.org/10.1007/s11721-007-0004-y

[19] Y. Gao, W.-H. Chen, and Z. Lu, "Kinematics analysis and experiment of a cockroach-like robot," *Journal of Shanghai Jiaotong University (Science)*, vol. 16, pp. 71–77, 2011. doi: 10.1007/s12204-011-1097-4

[20] Y. Bar-Cohen and C. Breazeal, "Biologically inspired intelligent robots," in *Proc. Smart Structures and Materials 2003: Electroactive Polymer Actuators and Devices (EAPAD)*, 2003, vol. 5051, pp. 14–20. doi: 10.1117/12.484379

[21] M. Brambilla, "Swarm robotics: A review from the swarm engineering perspective," *Swarm Intelligence*, vol. 7, pp. 1–41, 2013. doi: 10.1007/s11721-012-0075-2

[22] L. Pitonakova, R. Crowder, and S. Bullock, "Information exchange design patterns for robot swarm foraging and their application in robot control algorithms," *Frontiers in Robotics and AI*, vol. 5, 47, 2018. doi: 10.3389/frobt.2018.00047

[23] M. R. Cutkosky, "Bioinspired robot design," in *Robotics Goes MOOC: Design*, Cham, Switzerland: Springer, 2025, pp. 273–298, doi: 10.1007/978-3-319-75823-7_6

[24] Y. Wang, R. Othayoth, and C. Li, "Cockroaches adjust body and appendages to traverse cluttered large obstacles," *Journal of Experimental Biology*, vol. 225, no. 10, jeb243605, 2022. doi: 10.1242/jeb.243605

[25] S. Na, "Bio-inspired artificial pheromone system for swarm robotics applications," *Adaptive Behavior*, vol. 29, no. 4, pp. 395–415, 2021. doi: 10.1177/1059712320918936

[26] Q. Xin, "Advanced bio-inspired mechanical sensing technology: Learning from nature but going beyond nature," *Advanced Materials Technologies*, vol. 8, no. 1, 2200756, 2023, doi: 10.1002/admt.202200756

[27] M. K. Habib, K. Watanabe, and K. Izumi, "Biomimetics robots from bio-inspiration to implementation," in *Proc. IECON 2007-33rd Annual Conference of the IEEE Industrial Electronics Society*, IEEE, 2007. doi: 10.1109/IECON.2007.4460382

[28] C. Weinreb, "Keypoint-MoSeq: Parsing behavior by linking point tracking to pose dynamics," *Nature Methods*, vol. 21, no. 7, pp. 1329–1339, 2024. doi: 10.1038/s41592-024-02318-2

[29] V. A. Webster-Wood, "Biohybrid robots: Recent progress, challenges, and perspectives," *Bioinspiration & Biomimetics*, vol. 18, no. 1, 015001, 2022. doi: 10.1088/1748-3190/ac9c3b

[30] M. Katebi, "Challenges and trends of implantable functional electrical neural stimulators: System architecture and parameters," *IEEE Access*, 2024, doi: 10.1109/ACCESS.2024.3432611

[31] V. Panyam, "Bio-inspired design for robust power grid networks," *Applied Energy*, vol. 251, 113349, 2019. doi: 10.1016/j.apenergy.2019.113349

[32] C. Blum and R. Groß, "Swarm intelligence in optimization and robotics," in *Springer Handbook of Computational Intelligence*, pp. 1291–1309, 2015. doi: 10.1007/978-3-662-43505-2_66

[33] B. J. Fogg, "A behavior model for persuasive design," in *Proc. the 4th International Conference on Persuasive Technology*, 2009. doi: 10.1145/1541948.1541999

[34] R. J. Full and M. S. Tu, "Mechanics of six-legged runners," *Journal of Experimental Biology*, vol. 148, no. 1, pp. 129–146, 1990. doi: 10.1242/jeb.148.1.129

[35] D. L. Jindrich and R. J. Full, "Many-legged maneuverability: dynamics of turning in hexapods," *Journal of Experimental Biology*, vol. 202, no. 12, pp. 1603–1623, 1999. doi: 10.1242/jeb.202.12.1603

[36] J. A. Bender, "Kinematic and behavioral evidence for a distinction between trotting and ambling gaits in the cockroach *Blaberus discoidalis*," *Journal of Experimental Biology*, vol. 214, no. 12, pp. 2057–2064, 2011. doi: 10.1242/jeb.056481